Polímeros
ISSN 1678-5169 (Online)

https://doi.org/10.1590/0104-1428.20250016

ORIGINAL ARTICLES

Sustainable heterophasic ethylene-propylene copolymer composites with recycled aircraft graphite for antistatic packaging

Ágatha Missio da Silva[1] , Erick Gabriel Ribeiro dos Anjos[1], Thaís Ferreira da Silva[1], Rieyssa Maria de Almeida Corrêa[1] , Thiely Ferreira da Silva[1], Juliano Marini[2] and Fabio Roberto Passador[1]*

[1]Laboratório de Tecnologia em Polímeros e Biopolímeros – TecPBio, Departamento de Ciência e Tecnologia, Universidade Federal de São Paulo – UNIFESP, São José dos Campos, SP, Brasil

[2]Departamento de Engenharia de Materiais, Universidade Federal de São Carlos – UFSCar, São Carlos, SP, Brasil

**fabio.passador@unifesp.br*

Abstract

Antistatic packaging prevents electrostatic discharge (ESD) damage, protecting electronic components during storage and transport, ensuring reliability in industries like electronics and aerospace. This study develops heterophasic ethylene-propylene copolymer (HEPC) composites reinforced with recycled aircraft graphite for antistatic applications. HEPC composites with 1, 5, and 10 wt% recycled graphite were prepared via twin-screw extrusion and injection molding. Morphological, thermal, rheological, mechanical, and electrical properties were analyzed. Adding 5 wt% graphite increased the elastic modulus by 21.3% and Shore D hardness by 6.1%. Electrical conductivity improved significantly, with a nine-order magnitude increase for 5 wt% graphite, enabling effective electrostatic dissipation. This sustainable approach enhances material performance while promoting circular economy practices by upcycling aerospace waste into high-value functional materials.

Keywords: *composites, heterophasic ethylene-propylene copolymer, recycled graphite, antistatic packaging.*

Data Availability: Research data is available upon request from the corresponding.

How to cite: Silva, Á. M., Anjos, E. G. R., Silva, T. F., Corrêa, R. M. A., Silva, T. F., Marini, J., & Passador, F. R. (2025). Sustainable heterophasic ethylene-propylene copolymer composites with recycled aircraft graphite for antistatic packaging. *Polímeros: Ciência e Tecnologia*, *35*(3), e20250030. https://doi.org/10.1590/0104-1428.20250016

1. Introduction

Antistatic packaging is designed to prevent the accumulation of electrostatic charges, protecting sensitive electronic components and devices from electrostatic discharge (ESD)-induced damage[1]. These packaging materials can be conductive, dissipative, or coated with antistatic agents to control charge buildup, ensuring safe handling and transportation. Commonly used in the electronics and aerospace industries, antistatic packaging plays a crucial role in maintaining the integrity and functionality of electronic circuits, semiconductors, and other static-sensitive materials[2]. With technological advancements and the increasing consumption of electronic devices, proper packaging for transportation and storage has become even more critical. A significant challenge in this context is electrostatic discharge (ESD), which can occur due to friction between an electronic component and its packaging. ESD can damage these components, potentially causing small explosions that result in permanent loss of functionality[3]. Detecting and repairing ESD-related damage is often unfeasible due to the high costs involved, significantly contributing to electronic waste and increasing both financial and environmental burdens[4,5]. To address this issue, antistatic packaging has been developed to protect electronic components by dissipating static charges in a controlled manner[6].

In recent decades, polymers have emerged as competitive alternatives to traditional packaging materials due to their low density, cost-effective production, and ease of processing[7]. The most commonly used polymers for antistatic packaging are polyethylene (PE), polypropylene (PP), polyamide 6 (PA6), and polystyrene (PS), which exhibit high electrical resistivity, acting as electrical insulators and hindering the electrostatic charge dissipation[8,9].

To be used as antistatic packaging, polymers must not only meet mechanical requirements but also exhibit low electrical resistivity[10]. Since most polymers inherently have high electrical resistivity, it is necessary to incorporate antistatic agents, which are electrically conductive components. Among the most widely researched antistatic agents are graphene and graphene-related materials (GRM)[11], semiconducting

ceramic particles[6], conductive carbon black[12], graphite[13], and carbon nanotubes (CNT)[14]. The incorporation of recycled conductive fillers, such as graphite, into polymer matrices offers a sustainable approach to developing high-performance antistatic packaging solutions[13].

Graphite exhibits outstanding properties, including high electrical conductivity, chemical stability in high-temperature and non-oxidizing environments, significant resistance to thermal shocks, and favorable characteristics for mechanical processing. This work proposes the use of heterophasic ethylene-propylene copolymer (HEPC) as a polymeric matrix. HEPC stands out due to its excellent mechanical properties, such as tensile strength and impact resistance. Additionally, it offers the advantage of being more cost-effective compared to engineering polymers[15]. Graphite was incorporated as an antistatic agent to reduce electrical resistivity and achieve the required properties for antistatic packaging applications, characterizing the material as a polymer matrix composite (PMC)[16,17].

Polymer matrix composites (PMCs) are widely used in various technological fields, particularly in the aerospace industry. Their increasing demand in this sector is primarily due to their excellent strength-to-weight ratio, which enhances fuel efficiency and reduces operational costs. On average, commercial aircraft have a lifespan of approximately 20 years, and PMCs constitute around 18.7% of the materials used in their construction. As material advancements continue, this percentage is expected to increase, making the recovery of these composites increasingly important. In this study, mechanical recycling was employed to recover graphite from aircraft waste[18].

Zaggo et al.[13] investigated the use of recycled graphite as an antistatic agent in poly(trimethylene terephthalate) (PTT) composites for antistatic packaging. The authors incorporated recycled graphite into PTT at concentrations ranging from 1 to 20 wt%, with and without a compatibilizer agent (PTT-*g*-MA), processed by melt extrusion. The findings showed that adding 10 wt% of recycled graphite significantly reduced the electrical resistivity of PTT, making the composite suitable for antistatic applications. The study emphasized the potential of recycled graphite to improve the electrical, thermal, and mechanical properties of polymer composites while promoting sustainability.

Panwar et al.[19] analyzed the dielectric and electromagnetic interference (EMI) shielding properties of polypropylene (PP)-graphite composites. The results indicated that the composites follow the percolation theory model, with the percolation threshold occuring at approximately 5wt% of graphite, beyond which the composites exhibit nearly ohmic behavior. Additionally, the dielectric constant and dissipation factor significantly increases at low and radio frequencies, suggesting potential applications in electromagnetic shielding and electronic devices.

In this work, antistatic packaging based on HEPC with varying contents of recycled graphite from aerospace components was developed. The influence of different graphite contents (1, 5, and 10 wt%) on the rheological, thermal, mechanical, and electrical properties of the HEPC-graphite composites was analyzed, highlighting the potential for developing sustainable, high-performance materials for advanced packaging solutions. The results not only demonstrate significant improvements in material properties but also provide a pathway for integrating recycled aerospace waste into valuable, functional applications, offering both environmental and technological benefits.

2. Materials and Methods

2.1 Materials

Heterophasic ethylene-propylene copolymer (HEPC) specified as ES 540S, with a melt flow index of 42 g/10 min (230 °C/2.16 kg) and a density of 0.90 g/cm^3 was supplied by Braskem (Brazil). The recycled graphite was supplied by companies from Vale do Paraíba region (Brazil) as components of the aerospace sector. The pieces were ground, and the resulting powder was purified and characterized.

2.2 Composites preparation and processing

Firstly, the recycled graphite powder was subjected to heat treatment in a tubular furnace (EDG) at 1100°C, with a heating rate of 20°C/min, held for 2 hours under a nitrogen atmosphere, and then cooled at a controlled rate of 30 °C/min to remove residual oils from the aerospace components. The particle size of the powder was homogenized using a 100-mesh sieve.

HEPC composites with different recycled graphite contents (1, 5, and 10 wt%) were prepared by melt mixing method in a co-rotating twin-screw mini extruder from AX Plásticos (model AX16:40DR), with L/D = 40 mm, D = 16 mm and maximum material flow rate of 2 kg/h. The temperature profile was 225/230/240/240/245 ºC, and the feeding and screw speeds were 15 and 80 rpm, respectively. The nomenclature used for the compositions is based on the recycled graphite content. For example, HEPC/1% graphite refers to a composition containing 1 wt% of recycled graphite.

After the extrusion process, the composite filaments were cooled in a water bath at room temperature, pelletized, and then dried in a vacuum oven at 60 °C for 4 hours. Finally, the pellets were injection-molded using a vertical injection molding hot press (manufactured by MH Equipamentos, Brazil) with a barrel temperature of 255 °C, an injection mold pressure of 8 bar, and a mold temperature of 50 °C. The composites were molded in an aluminum injection mold into Type I tensile test specimens, according to ASTM D638-18[20], and Izod impact strength test specimens, according to ASTM D256-06[21].

2.3 Characterizations of recycled graphite, HEPC and composites

2.3.1 Morphological characterization of the recycled graphite, HEPC and composites

The morphologies of the recycled graphite, HEPC, and the composites were analyzed using scanning electron microscopy (SEM) with an Inspect S50 (FEI Company) microscope, equipped with secondary electron (SE) detectors. It was operated at 5 keV, and the samples were placed on aluminum stubs and coated with a thin layer of gold using sputtering.

2.3.2 Rheological characterization

The tests in the steady shear and oscillatory regimes were performed using the ARG2 controlled stress rheometer (TA Instruments), with parallel plate geometry of 25 mm diameter and distance between plates of 1.0 mm, at 250 °C under a nitrogen atmosphere (N_2). The viscoelastic properties of complex viscosity (η*), storage modulus (G'), and loss modulus (G'') were analyzed as a function of angular frequency. For the oscillatory tests, strain sweep tests were performed to select a strain amplitude within the linear viscoelastic range (0.5% for all samples).

2.3.3 Electrical characterization

The impedance spectroscopy measurements were conducted using a Solartron SI 1260 impedance analyzer from AMETEK Scientific Instruments, operated at 25 °C and a voltage amplitude of 0.5 V. The volumetric electrical conductivity on alternating current (AC) and the complex permittivity (ε*) were evaluated at the frequency range of 1 to 10^6 Hz.

The samples were prepared by hot pressing the material between two metal plates, prepared with Chemlease® 41-90 EZ release agent from Chem-Trend. The press used was from MH Equipamentos, model PR8HP. Then, a thin layer of a Gold-Palladium (Au-Pd) alloy was deposited on the faces of the samples as electrodes using the sputtering process. This process was performed in a Q150R ES metallizer from Quantum, with a metalization time of 90s and a current of 20 mA.

2.3.4 Thermal characterization

The thermal behavior of the samples was evaluated using differential scanning calorimetry (DSC) with a TA Instruments Q2000 equipment, operating with nitrogen as the carrier gas at a constant flow rate of 50 mL/min. The samples underwent a thermal cycle consisting of heating at 10 °C/min from -20 °C to 250 °C, where they were held for 3 minutes to eliminate thermal history. Subsequently, they were cooled at 10 °C/min from 250 °C to -20 °C and then reheated at the same rate for a second heating cycle up to 250 °C.

The degree of crystallinity (X_c) was calculated based on the corrected enthalpy of fusion (ΔHm^{corr}) of the samples and the standard enthalpy of PP when it is 100% crystalline (ΔHm^o = 190 J/g)[15]. ΔHm^{corr} were considered based on the graphite content (ϕ) in the samples, since the measured ΔHm refers only to the neat polymer.

$$Xc = \left[\frac{\Delta Hm}{(1 - \quad) \times \Delta Hm^o} \right] \times 100 = \left(\frac{\Delta Hm^{corr}}{\Delta Hm^o} \right) \times 100 \qquad (1)$$

2.3.5 Mechanical characterization

Shore D Hardness Test: The average hardness of each composition was obtained through the Shore D hardness test at 9 different points on the surface of the specimen using a portable digital durometer (Instrutherm, model DP 400), according to ASTM D2240[22].

Tensile Tests: The tests were performed on an MTS machine, model Criterion 45, with a crosshead speed of 50 mm/min and a load cell with a maximum capacity of 50 kN. For each composition, 5 samples were tested according to ASTM D638-18[20].

Izod Impact Strength: A CEAST/Instron Izod impact test machine, model 9050, coupled with a 1.0 J hammer was used to perform the tests. Five samples of each composition were tested according to ASTM D256-06[21]. For the test, the samples were notched with a 0.1-inch depth notch using a manual notching machine.

Statistical Analysis: A one-way analysis of variance (ANOVA) followed by a post-hoc Tukey HSD test to compare pairs at α = 0.05 of significance were executed on the mechanical properties data.

3. Results and Discussions

3.1 Recycled graphite characterization

Figure 1 shows the SEM image of recycled graphite. A homogeneous surface is observed, indicating the compaction of the graphite. This suggests that the applied thermal treatment effectively prevented graphite dispersion by removing residual surface impurities. As discussed by Zaggo et al.[13], the removal of these impurities significantly enhances the graphite structure, improving its properties and ensuring greater stability and performance.

3.2 Morphology of the HEPC and composites

The morphology of the HEPC exhibited a heterogeneous structure, with visible cavities within a more continuous matrix, likely indicating PE domains dispersed throughout the PP matrix (Figure 2a). Due to the high immiscibility of these two blocks[23], the secondary PE domains may contribute to the stiffness of the PP. Notably, these domains are not spherical, as would typically be observed in a PE/PP polymer blend[24], suggesting a distinct morphological interaction specific to the block copolymer.

In composites containing 1, 5, and 10 wt% recycled graphite, initial observations at 1wt% revealed only a few graphite fragments within the analyzed region of the matrix. However, as the concentration increased to 5 and 10 wt%,

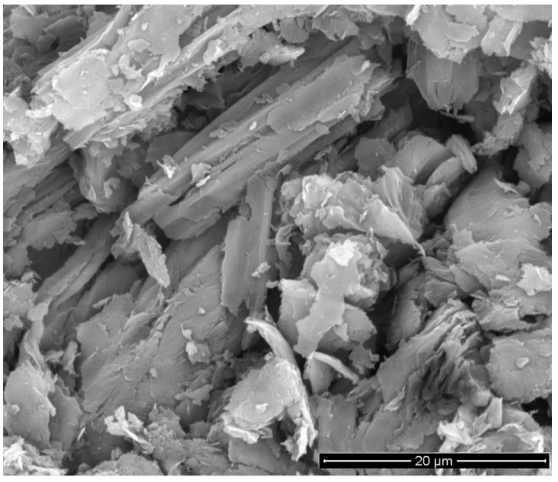

Figure 1. SEM image of recycled graphite, with a magnification of 6,000×.

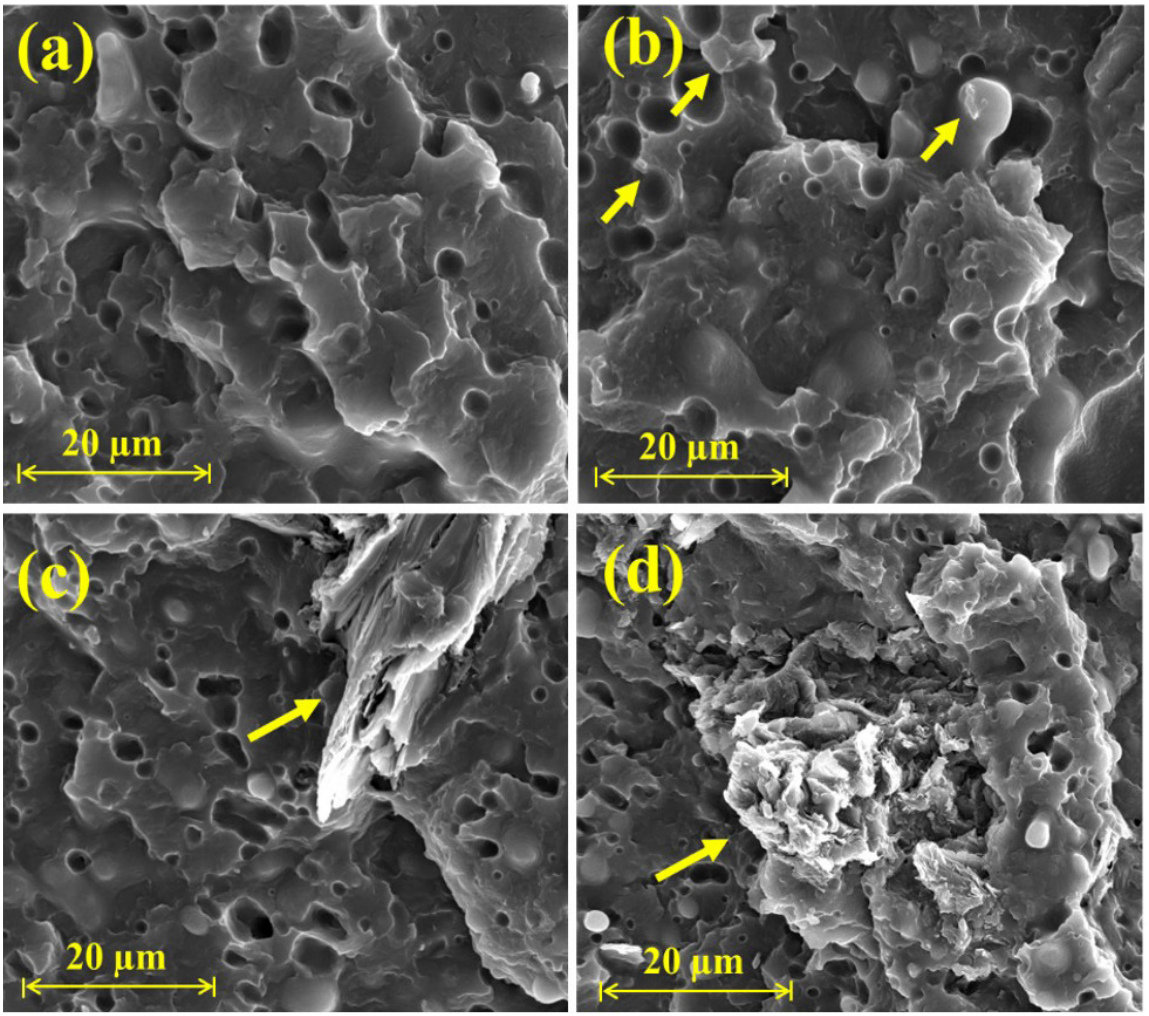

Figure 2. SEM micrographs of (a) HEPC, (b) HEPC/1%graphite, (c) HEPC/5%graphite, and (d) HEPC/10%graphite.

larger agglomerates of ground-recycled graphite were observed, and the layered structure of ground-recycled graphite became evident. The coarse morphology and agglomerate formation differed from previous findings in PTT-recycled graphite composites, likely due to the heterogeneous nature of the HEPC matrix. This structure could potentially be improved with the addition of a compatibilizer agent, as suggested by Zaggo et al.[13].

3.3 Rheological behavior of the HEPC and composites

The rheological behavior of the composites was studied in the oscillatory regime to better understand their viscoelastic properties and their relationship with morphological features (Figure 3a-c). Additionally, rotational testing in the steady-state regime was conducted to evaluate flow behavior at low shear rates (Figure 3d). The HEPC copolymer exhibited a low complex viscosity (10^3 to 10^2 Pa·s), with a significant decrease in the terminal angular frequency range (10^{-2} to 10^0 rad/s). This drop may be attributed to the stiffer PP chain segments within the heterogeneous copolymer structure. As expected, a liquid-like behavior was observed, with the loss modulus exceeding the storage modulus across most angular frequencies. Notably, the Cox-Merz rule did not apply to this copolymer, which may be related to phase separation[25], as evidenced by differing behaviors between complex and steady-state viscosity in the terminal region, where the more structured chain features were not visible at low shear rates.

Literature suggests that adding graphite powder to a polymer matrix can create a lubricating effect, facilitating the slippage of polymer chains along the graphite surface and improving flow[26]. This effect was particularly pronounced in the PP segments, where higher graphite concentrations (5 and 10 wt%) led to a reduction in complex viscosity, primarily by decreasing the storage modulus at low frequencies. Despite these changes, the overall viscosity remained largely unaffected by graphite concentration - a favorable outcome for its use as a filler, as it does not compromise the processability of the polymer.

3.4 Electrical characterization of the HEPC and composite films

The intrinsic conductivity of graphite arises from its sp^2-hybridized hexagonal lattice structure[13]. Consequently,

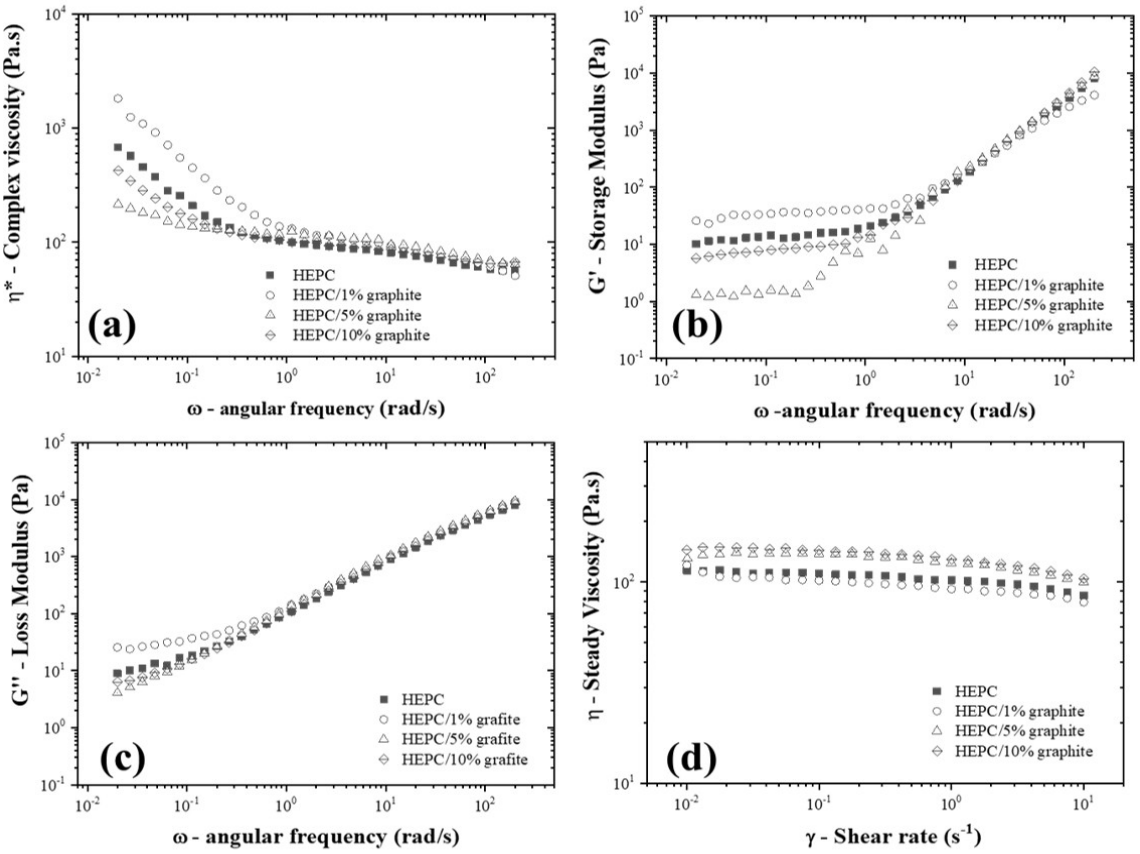

Figure 3. SAOS rheological behavior: (a) complex viscosity, (b) storage modulus, and (c) Loss modulus. (d) Steady-state viscosity obtained by rotational test.

incorporating graphite fragments into a polymer matrix may enhance its electrical conductivity, providing potential benefits for applications such as electrostatic discharge (ESD) protection. AC volumetric electrical conductivity of the films was measured via impedance spectroscopy (Figure 4). The PE/PP block copolymer exhibited typical insulating behavior, with electrical conductivity values below 10^{-10} S/cm and a frequency-dependent response attributed to variations in electric field incidence.

Adding 1 wt% graphite did not significantly impact the electrical conductivity of the polymer. However, compositions with 5 wt% and 10 wt% graphite exhibited similar electrical conductivity profiles, dramatically increasing around six orders of magnitude and transitioning to semiconducting behavior suitable for ESD applications, with electrical conductivity around 10^{-3} S/cm[12]. Two key factors are noteworthy: first, the film form of the samples, which, as observed in a previous study[27], can lead to higher electrical conductivity values for carbon-based materials; and second, the measurement of volumetric rather than surficial conductivity, which may be more relevant for ESD applications. In certain carbon-based nanocomposites, such as those containing carbon black and higher filler contents, volumetric and surface conductivity values can often converge. Given the obtained electrical conductivity values, composites with

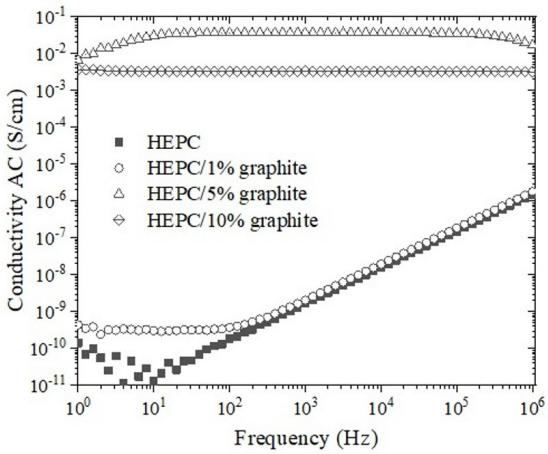

Figure 4. Volumetric electrical conductivity of the films with 0.2 mm thickness.

5 wt% and 10 wt% recycled graphite are suitable for use in antistatic packaging.

3.5 Thermal characterization of HEPC and composites

Figure 5 shows the DSC curves obtained during the first heating, cooling, and second heating stages, while

the thermal analysis results are summarized in Table 1. No significant difference was observed in the melting temperature (Tm_1 = 169°C, Tm_2 = 163°C) between the samples. This may suggest that graphite addition had no significant influence on the melting behavior of the HEPC matrix. This conclusion is further supported by the heating curves of all composites, which were nearly identical. Comparing the HEPC sample with the composites reinforced with graphite, a 3°C increase in the crystallization temperature was observed in the HEPC/10% graphite sample. The addition of graphite slightly reduced the degree of crystallinity of the composites from 38% to 34%, depending on the recycled graphite content, suggesting that graphite may act as a barrier to crystallite growth. Similar results were observed by Sarturato et al.[15] in their study on polypropylene/talc hybrid composites with graphene nanoplatelets (GNP). It is important to highlight that the same polymer matrix was used, and the decision to use the enthalpy of fusion value for the 100% crystalline PP sample was made to ensure a consistent comparison within the studied samples.

3.6 Mechanical characterization of HEPC and composites

Table 2 presents the mechanical properties of the samples, and Figure 6A shows the stress-strain curves. The ultimate tensile strength (UTS), deformation at the break, elastic modulus (E), Shore D hardness, and impact strength were statistically analyzed. Table 2 highlights the statistical differences when comparing the composites with HEPC, with results showing significant differences ($p < 0.001$). Figure 7 shows the comparative results for elastic modulus and Shore D hardness, accompanied by ANOVA analysis.

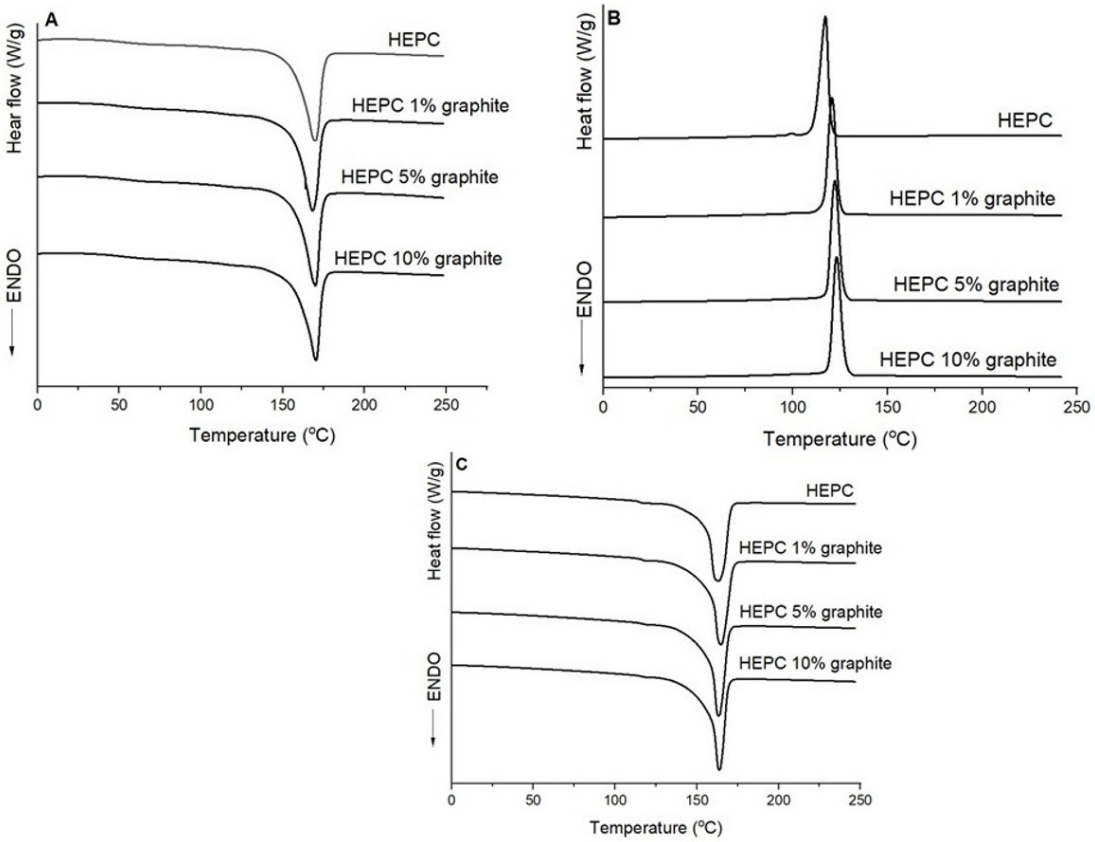

Figure 5. Differential scanning calorimetry curves (A) first heating, (B) cooling, and (C) second heating of the HEPC and HEPC composites with 1, 5, and 10 wt% of recycled graphite.

Table 1. Thermal properties obtained from DSC heating curves of the first heating scan, cooling, and second heating scan for HEPC and HEPC composites with 1, 5, and 10 wt% recycled graphite.

Sample	Tm_1 (°C)	ΔHm_1 (J/g)	Tc (°C)		Tm_2 (°C)	ΔHm_2 (J/g)	Xc (%)
HEPC	169	72	117	163	79		38
HEPC/1% graphite	169	74	121	163	82		36
HEPC/5% graphite	169	73	121	163	81		36
HEPC/10% graphite	169	71	122	163	80		34

Table 2. Mechanical properties of HEPC and HEPC composites with different graphite contents.

Samples	Ultimate tensile strength (MPa)	Elastic modulus (MPa)	Deformation at break (%)	Hardness (Shore D)	Impact strength (J/m)
HEPC	18.8 ± 1.8[a]	807.2 ± 64.7[a]	6.0 ± 0.9[a]	64.8 ± 4.7[a]	31.8 ± 3.8[a]
HEPC/1% graphite	18.4 ± 2.2[a]	867.9 ± 66.7[a]	4.4 ± 1.0[b]	69.9 ± 1.7[b]	31.5 ± 5.1[a]
HEPC/5% graphite	18.6 ± 1.2[a]	979.7 ± 38.7[b]	4.1 ± 0.6[b]	69.4 ± 2.7[b]	30.4 ± 3.6[a]
HEPC/10% graphite	18.5 ± 0.8[a]	995.5 ± 14.1[b]	4.2 ± 0.7[b]	70.9 ± 1.1[b]	29.6 ± 2.6[a]

Mean values followed by the same letter do not differ according to the Tukey–Kramer test at a 0.05 significance level.

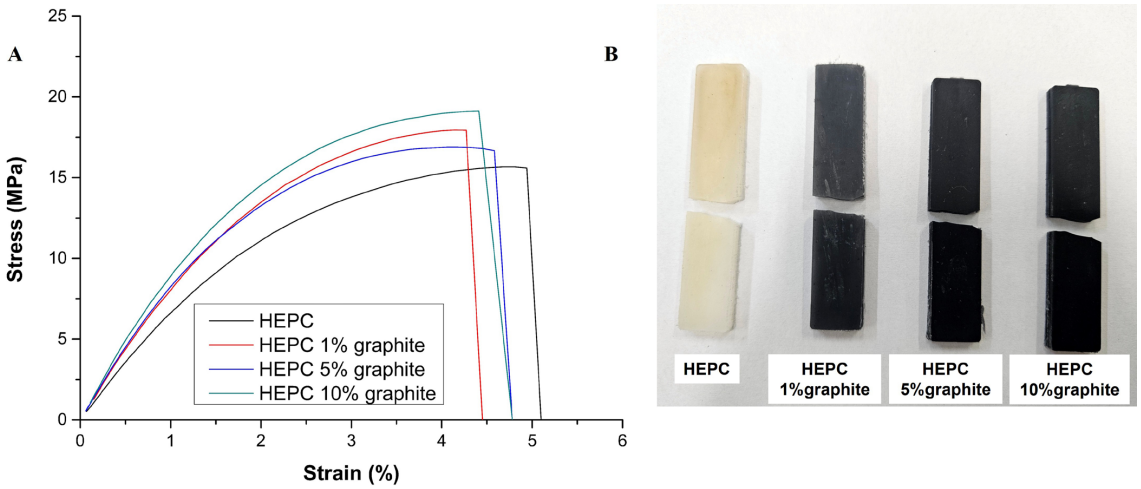

Figure 6. (A) Stress–strain curves and (B) specimens after Izod impact resistance test for HEPC and HEPC composites with different graphite contents.

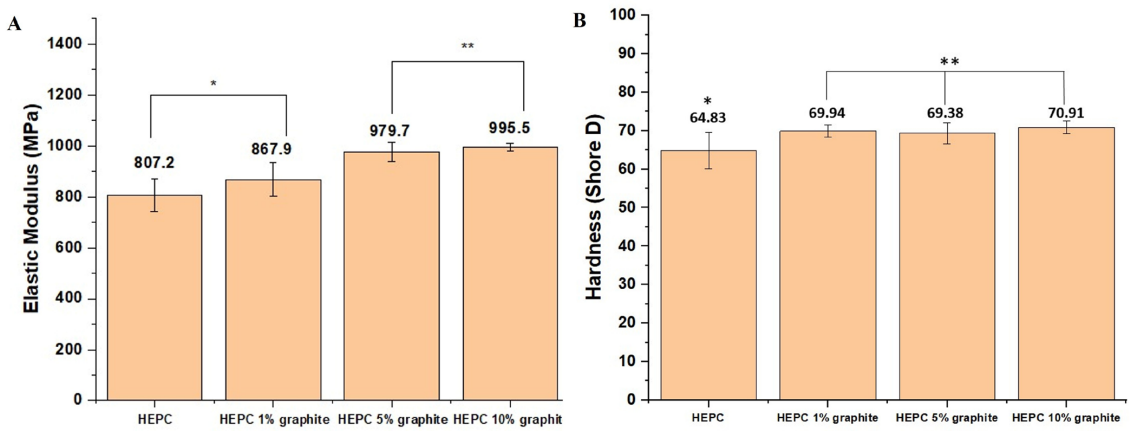

Figure 7. Mechanical test results: (A) Elastic modulus and (B) Shore D Hardness for HEPC and HEPC composites with different graphite contents. Results are given as mean ± standard deviation. Asterisks (*) indicate statistical significance (*$p \leq 0.01$; ** $p \leq 0.001$).

The incorporation of 10 wt% of recycled graphite resulted in a 23.3% increase in elastic modulus compared to the HEPC matrix, representing the best performance among the samples analyzed. Additionally, the addition of 1 wt% and 5 wt% of recycled graphite also showed promising results, increasing elastic modulus by 7.5% and 21.3%, respectively, compared to HEPC. This behavior can be attributed to the high intrinsic stiffness of graphite, which restricts the mobility of polymer chains. Consequently, the increase in elastic modulus led to a reduction in deformation at break with the addition of graphite.

Regarding tensile strength, represented by the ultimate tensile strength (UTS), the composites exhibited slight variations, with all samples showing similar values. This indicates that the addition of recycled graphite (1, 5, and 10 wt%) did not have a significant impact on the UTS.

An analysis of the Shore D hardness results reveals that incorporating graphite into the HEPC matrix led to an approximately 10% increase in Shore D hardness. However, varying the graphite concentration between 1, 5, and 10 wt% did not significantly affect this increase, as all three concentrations exhibited similar hardness values. Considering the standard deviation, the value obtained for the copolymer was comparable to that reported by Alfaro et al. [28]. Regarding impact resistance, the results indicate that the addition of recycled graphite (1, 5, and 10 wt%) did not significantly affect the impact strength of HEPC composites, with values remaining close to those of the neat material (HEPC). Therefore, at the studied concentrations and processing conditions, graphite incorporation does not compromise the impact resistance of the composites, which may be advantageous for applications where maintaining this property is essential.

As expected, the fracture type was identified as brittle for all analyzed compositions, a characteristic behavior of propylene. The fracture of the samples (Figure 6B) occurred at approximately half their length during the Izod impact strength test, indicating that the HEPC composite with recycled graphite has a homogeneous distribution and uniform mechanical properties. This suggests that the manufacturing process was efficient, and that the addition of graphite did not compromise the structural integrity of the material.

4. Conclusions

Heterophasic ethylene-propylene copolymer (HEPC) composites with varying levels of recycled graphite were successfully produced by extrusion. The resulting properties suggest that this material is suitable for use as antistatic packaging.

The morphological analysis indicated that the composition containing 1 wt% of graphite exhibited good particle dispersion, suggesting a homogeneous distribution in the polymer matrix. However, with an increase in graphite content from 5% to 10 wt%, agglomerations were observed, suggesting that dispersion becomes less efficient at higher concentrations. The addition of recycled graphite slightly decreased the degree of crystallinity of the composites from 38% to 34%, according to the added graphite content, indicating that graphite could act as a possible barrier to crystallite growth.

Regarding mechanical properties, the addition of recycled graphite significantly increased the elastic modulus and Shore D hardness compared to the neat copolymer. However, it led to a slight reduction in tensile strength and Izod impact resistance. Additionally, electrical properties through impedance spectroscopy testing showed that incorporating recycled graphite significantly enhanced the electrical conductivity of the composite, thereby decreasing its electrical resistivity and making it suitable for antistatic packaging applications.

Among the studied compositions, the addition of 5 wt% of recycled graphite resulted in the best balance, improving mechanical properties while ensuring sufficient electrical resistivity for antistatic packaging use.

5. Author's Contribution

- **Conceptualization –** Fabio Roberto Passador.
- **Data curation –** Fabio Roberto Passador.
- **Formal analysis –** Ágatha Missio da Silva; Erick Gabriel Ribeiro dos Anjos; Thaís Ferreira da Silva; Rieyssa Maria de Almeida Corrêa; Thiely Ferreira da Silva; Juliano Marini.
- **Funding acquisition –** Fabio Roberto Passador.
- **Investigation –** Ágatha Missio da Silva.
- **Methodology –** Ágatha Missio da Silva.
- **Project administration –** Fabio Roberto Passador.
- **Resources –** Fabio Roberto Passador.
- **Software –** NA.
- **Supervision –** Fabio Roberto Passador.
- **Validation –** Erick Gabriel Ribeiro dos Anjos; Thaís Ferreira da Silva; Rieyssa Maria de Almeida Corrêa; Thiely Ferreira da Silva.
- **Visualization –** Juliano Marini.
- **Writing – original draft –** Ágatha Missio da Silva.
- **Writing – review & editing –** Erick Gabriel Ribeiro dos Anjos; Thaís Ferreira da Silva; Rieyssa Maria de Almeida Corrêa; Thiely Ferreira da Silva; Juliano Marini; Fabio Roberto Passador.

6. Acknowledgements

The authors are grateful to FAPESP (Fundação de Amparo à Pesquisa do Estado de São Paulo, process 2024/11092-8) and CNPq (Conselho Nacional de Desenvolvimento Científico e Tecnológico, process 307933/2021-0) for financial support. The authors also thank the company Lyondell Basell for the donation of HEPC.

7. References

1. Silva, T. F., Menezes, F., Montagna, L. S., Lemes, A. P., & Passador, F. R. (2018). Preparation and characterization of antistatic packaging for electronic components based on poly(lactic acid)/carbon black composites. *Journal of Applied Polymer Science*, *136*(13), 47273. http://doi.org/10.1002/app.47273.
2. Vieira, L. S., Anjos, E. G. R., Verginio, G. E. A., Oyama, I. C., Braga, N. F., Silva, T. F., Montagna, L. S., & Passador, F. R. (2022). A review concerning the main factors that interfere in the electrical percolation threshold content of polymeric antistatic packaging with carbon fillers as antistatic agent. *Nano Select*, *3*(2), 248-260. https://www.doi.org/10.1002/nano.202100073.
3. Singh, S., & El-Khateeb, H. (1994). Evaluation of a proposed test method to measure surface and volume resistance of static dissipative packaging materials. *Packaging Technology & Science*, *7*(6), 357-362. http://doi.org/10.1002/pts.2770070605.

4. Mojzes, Á., Tóth, B., & Csavada, P. (2014). Investigation of an electrostatic discharge protective biodegradable packaging foam in the logistic chain. *Logistics, Supply Chain, Sustainability and Global Challenges*, *5*(1), 25-33. https://www.doi.org/10.1515/jlst-2015-0004.
5. Santos, M. S., Montagna, L. S., Rezende, M. C., & Passador, F. R. (2019). A new use for glassy carbon: development of LDPE/glassy carbon composites for antistatic packaging applications. *Journal of Applied Polymer Science*, *136*(11), 47204. http://doi.org/10.1002/app.47204.
6. Zhou, Y., Wang, H., Wang, L., Yu, K., Lin, Z., He, L., & Bai, Y. (2012). Fabrication and characterization of aluminum nitride polymer matrix composites with high thermal conductivity and low dielectric constant for electronic packaging. *Materials Science and Engineering B*, *117*(11), 892-896. http://doi.org/10.1016/j.mseb.2012.03.056.
7. Huang, H.-D., Ren, P.-G., Zhong, G.-J., Olah, A., Li, Z.-M., Baer, E., & Zhu, L. (2023). Promising strategies and new opportunities for high barrier polymer packaging films. *Progress in Polymer Science*, *144*, 101722. http://doi.org/10.1016/j.progpolymsci.2023.101722.
8. Lee, J.-I., Yang, S.-B., & Jung, H.-T. (2009). Carbon nanotubes−polypropylene nanocomposites for electrostatic discharge applications. *Macromolecules*, *42*(21), 8328-8334. http://doi.org/10.1021/ma901612w.
9. Rousseaux, D., Lhost, O., & Lodefier, P. (2013). *Industrial advanced carbon nanotubes-based materials for electrostatic discharge packaging*. In *Proceedings of the 14th International Conference on Electronic Packaging Technology (ICEPT)* (pp. 386-388). USA: IEEE. http://doi.org/10.1109/ICEPT.2013.6756495.
10. Vieira, L. S., Anjos, E. G. R., Verginio, G. E. A., Oyama, I. C., Braga, N. F., Silva, T. F., Montagna, L. S., Rezende, M. C., & Passador, F. R. (2021). Carbon-based materials as antistatic agents for the production of antistatic packaging: a review. *Journal of Materials Science Materials in Electronics*, *32*(4), 3929-3947. http://doi.org/10.1007/s10854-020-05178-6.
11. Bhardwaj, P., & Grace, A. N. (2020). Antistatic and microwave shielding performance of polythiophene-graphene grafted 3-dimensional carbon fibre composite. *Diamond and Related Materials*, *106*, 107871. http://doi.org/10.1016/j.diamond.2020.107871.
12. Silva, L. N., dos Anjos, E. G. R., Morgado, G. F. M., Marini, J., Backes, E. H., Montagna, L. S., & Passador, F. R. (2020). Development of antistatic packaging of polyamide 6/linear lowdensity polyethylene blendsbased carbon black composites. *Polymer Bulletin*, *77*(7), 3389-3409. http://doi.org/10.1007/s00289-019-02928-3.
13. Zaggo, H. M., Braga, N. F., Anjos, E. G. R., Montagna, L. S., Antonelli, E., & Passador, F. R. (2022). Effect of recycled graphite as an antistatic agent on the mechanical, thermal, and electrical properties of poly(trimethylene terephthalate). *Macromolecular Symposia*, *406*(1), 2200014. http://doi.org/10.1002/masy.202200014.
14. Braga, N. F., LaChance, A. M., Liu, B., Sun, L., & Passador, F. R. (2019). Influence of compatibilizers and carbon nanotubes on mechanical, electrical and barrier properties of PTT/ABS blends. *Advanced Industrial and Engineering Polymer Research*, *2*(3), 121-125. https://doi.org/10.1016/j.aiepr.2019.07.002.
15. Sarturato, A. C. P., Anjos, E. G. R., Marini, J., Morgado, G. F. M., Baldan, M. R., & Passador, F. R. (2023). Polypropylene/talc/graphene nanoplates (GNP) hybrid composites: effect of GNP content on the thermal, rheological, mechanical, and electrical Properties. *Journal of Applied Polymer Science*, *140*(12), e53657. http://doi.org/10.1002/app.53657.
16. Peng, Q., Tan, X., Venkataraman, M., & Militky, J. (2022). Tailored expanded graphite based PVDF porous composites for potential electrostatic dissipation applications. *Diamond and Related Materials*, *125*, 108972. http://doi.org/10.1016/j.diamond.2022.108972.
17. Goyal, R. K., Jagadale, P. A., & Mulik, U. P. (2009). Thermal, mechanical, and dielectric properties of polystyrene/expanded graphite nanocomposites. *Journal of Applied Polymer Science*, *111*(4), 2071-2077. http://doi.org/10.1002/app.29042.
18. Ramawat, N., Sharma, N., Yamba, P., & Sanidhi, M. A. T. (2023). Recycling of polymer-matrix composites used in the aerospace industry—A comprehensive review. *MaterialsToday: Proceedings*. In Press. https://www.doi.org/10.1016/j.matpr.2023.05.386.
19. Panwar, V., Park, J.-O., Park, S.-H., Kumar, S., & Mehra, R. M. (2010). Electrical, dielectric, and electromagnetic shielding properties of polypropylene-graphite composites. *Journal of Applied Polymer Science*, *115*(3), 1306-1314. http://doi.org/10.1002/app.29702.
20. American Society for Testing and Materials – ASTM. (2003). *ASTM D638-03: standard test method for tensile properties of plastics*. West Conshohocken, PA: ASTM International.
21. American Society for Testing and Materials – ASTM. (2018). *ASTM D256: standard test methods for determining the Izod pendulum impact resistance of plastics*. West Conshohocken, PA: ASTM International; 2018.
22. American Society for Testing and Materials – ASTM. (2013). *ASTM D2240: standard test method for rubber property—durometer hardness*. West Conshohocken, PA: ASTM International.
23. De Rosa, C., Malafronte, A., Di Girolamo, R., Auriemma, F., Ruiz de Ballesteros, O., & Coates, G. W. (2020). Morphology of isotactic polypropylene−polyethylene block copolymers driven by controlled crystallization. *Macromolecules*, *53*(22), 10234-10244. http://doi.org/10.1021/acs.macromol.0c01316.
24. Jose, S., Parameswaranpilla, J., Francis, B., Aprem, A. S., & Thomas, S. (2016). Thermal degradation and crystallization characteristics of multiphase polymer systems with and without compatibilizer. *AIMS Materials Science*, *3*(3), 1177-1198. http://doi.org/10.3934/matersci.2016.3.1177.
25. Di, Y., Iannace, S., & Nicolais, L. (2002). Thermal behavior and morphological and rheological properties of polypropylene and novel elastomeric ethylene copolymer blends. *Journal of Applied Polymer Science*, *86*(13), 3430-3439. http://doi.org/10.1002/app.11371.
26. Zhang, H., Yang, Z., Su, K., Huang, W., & Zhang, J. (2022). Effects and mechanism of filler content on thermal conductivity of composites: a case study on plasticized polyvinyl chloride/graphite composites. *Journal of Polymer Engineering*, *42*(7), 599-608. http://doi.org/10.1515/polyeng-2021-0268.
27. Anjos, E. G. R., Brazil, T. R., Morgado, G. F. M., Antonelli, E., Rezende, M. C., Pessan, L. A., Moreira, F. K. V., Marini, J., & Passador, F. R. (2023). Renewable PLA/PHBV blend-based graphene nanoplatelets and carbon nanotube hybrid nanocomposites for electromagnetic and electric-related applications. *ACS Applied Electronic Materials*, *5*(11), 6165-6177. http://doi.org/10.1021/acsaelm.3c01099.
28. Alfaro, E. F. (2010). *Estudos da utilização de cinzas de casca de arroz como carga em matriz de polipropileno e do efeito da radiação ionizante sobre este compósito* (Dissertação de mestrado). Instituto de Pesquisas Energéticas e Nucleares, São Paulo. https://www.doi.org/10.11606/D.85.2010.tde-08082011-105312.

Received: Mar. 17, 2025
Revised: May 21, 2025
Accepted: May 24, 2025

Editor-in-Chief: Sebastião V. Canevarolo